026370-2-F

Final Report

Correlation of Infrasonic Microbarometric Disturbances and Long Period Seismic Phenomena

Period Covered: 1 February 1969, to 31 May 1971

PAUL W. POMEROY
MALCOLM J. S. JOHNSTON

June 1971

Air Force Office of Scientific Research
Contract No. F44620-69-C-0085
ARPA Order No. 1363
Arlington, Virginia

Department of Geology and Mineralogy
Seismological Observatory

Approved for public release; distribution unlimited.

41

Unclassified

Security Classification

DOCUMENT CONTROL DATA - R & D

(Security classification of title, body of abstract and indexing annotation must be entered when the overall report is classified)

1. ORIGINATING ACTIVITY (Corporate author)
The Regents of The University of Michigan
Department of Geology and Mineralogy
Ann Arbor, Michigan 48104

2a. REPORT SECURITY CLASSIFICATION
Unclassified

2b. GROUP

3. REPORT TITLE

CORRELATION OF INFRASONIC MICROBAROMETRIC DISTURBANCES AND LONG-PERIOD SEISMIC PHENOMENA

4. DESCRIPTIVE NOTES (Type of report and inclusive dates)
Scientific—Final (

5. AUTHOR(S) (First name, middle initial, last name)

Paul W. Pomeroy and Malcolm J.S. Johnston

6. REPORT DATE	7a. TOTAL NO. OF PAGES	7b. NO. OF REFS
June 1, 1971	39	---

8a. CONTRACT OR GRANT NO.	9a. ORIGINATOR'S REPORT NUMBER(S)
F44620-69-C-0085	026370-2-F
b. PROJECT NO. ARPA Order No. 1363	
c. Program Code No. 9F20	9b. OTHER REPORT NO(S) (Any other numbers that may be assigned this report)
d. 62701D	AFOSR - TR - 71-[illegible]

10. DISTRIBUTION STATEMENT

Approved for public release; distribution unlimited.

11. SUPPLEMENTARY NOTES	12. SPONSORING MILITARY ACTIVITY
TECH, OTHER	Air Force Office of Scientific Research 1400 Wilson Boulevard (NPG) Arlington, Virginia 22209

13. ABSTRACT

Detailed analyses of the correlation of infrasonic microbarometric disturbances and long-period seismic phenomena as recorded at the high-gain, wide-band, long-period seismic observatory at Sugar Island, Michigan, show very low coherency in the range of periods between 10 and 120 sec. At periods greater than 60 sec, rising levels of microbarometric power generally correspond to rising levels of seismic "noise" power indicating a genetic relationship. The lack of coherency between the data is attributed to the fact that a single point microbarometric measurement at the seismic recording site does not adequately represent the atmospheric loading of the earth's surface. To obtain high coherency, an array of weighted microbarometric measurements should be obtained in an area approximately 10 km in diameter around a broad-band, high-gain seismic receiver. A pronounced minimum in the seismic noise between 30 to 40 sec was observed in accordance with Savino's observations.

THE UNIVERSITY OF MICHIGAN

DEPARTMENT OF GEOLOGY AND MINERALOGY
Seismological Observatory

Final Report

Period Covered: 1 February 1969, to 31 May 1971

ARPA Order Number 1363

Program Code Number 9F20

Contractor: The Regents of The University of Michigan

Date of Contract: 1 February 1969

Amount of Contract: $108,450

Contract Expiration Date: 31 May 1971

Contract Number: F44620-69-C-0085

Principal Investigator: Paul W. Pomeroy (AC 313-764-8322)

Short Title: Correlation of Atmospheric and Seismic Waves

TABLE OF CONTENTS

LIST OF ILLUSTRATIONS

LIST OF ILLUSTRATIONS (Concluded)

ABSTRACT

Detailed analyses of the correlation of infrasonic microbarometric disturbances and long-period seismic phenomena as recorded at the high-gain, wide-band, long-period seismic observatory at Sugar Island, Michigan, show very low coherency in the range of periods between 10 and 120 sec. At periods greater than 60 sec, rising levels of microbarometric power generally correspond to rising levels of seismic "noise" power indicating a genetic relationship. The lack of coherency between the data is attributed to the fact that a single point microbarometric measurement at the seismic recording site does not adequately represent the atmospheric loading of the earth's surface. To obtain high coherency, an array of weighted microbarometric measurements should be obtained in an area approximately 10 km in diameter around a broad-band, high-gain seismic receiver. A pronounced minimum in the seismic noise between 30 to 40 sec was observed in accordance with Savino's observations.

INTRODUCTION

The work statement for this contract provides for studies of atmospheric and seismic phenomena as follows:

1. Investigate the correlation of infrasonic microbarometric disturbances and long-period seismic phenomena.

   A. in the vicinity of the earthquake epicenter;

   B. in the vicinity of the seismic and acoustic receivers; and

   C. due to coupling between Rayleigh waves and acoustic waves when the proper conditions exist, i.e., when the velocity of the surface seismic waves is less than the speed of sound in air.

2. To investigate the source and propagation characteristics of infrasonic phenomena other than those correlatable directly with seismic events. These include volcanic activity, rocket launches, tornado activities, magnetic storms, etc., all of which are associated with microbarometric activity.

Because of the great interest in the source of "noise" with periods greater than 30 sec on high-gain, wide-band seismographs, the work on this contract has been confined principally to Item 1 above. The "noise" in this period range together with the shorter period (i.e., 14-22 sec) oceanic wave-generated microseismic noise constitute the limiting factors in magnification on long-period seismographs at the present time. It would appear that at least two sets of long-period seismic instrumentation are capable of higher operational manifications than even those achieved by the current high-gain, wide-band, long-period network being installed by the Lamont Doherty Geological Observatory. These instruments include those described by Block, et al., and Pomeroy, et al. The 14-22-sec microseisms can be minimized by an appropriate choice of filters. If the longer period noise is atmospherically generated and coupled to the ground in the vicinity of the seismic receiver, then its elimination rests on the simultaneous recording of microbarometric information in the same period range. By appropriate normalization and subtraction of the microbarometric data from the long-period seismic data, increased useful magnifications may be achieved. As this research indicates, however, this may be achieved only with the recording of an array of microbarographs and the possibility becomes expensive at the very least.

If, on the other hand, part or all of the long-period noise is not coupled to the ground, then the elucidation of the source of this noise can result in the immediate increase in the achievable useful magnification of long-period seismographs. It was clearly shown in Annual Report No. 1

(02637-1-P), on this contract, that propagating long-period atmospheric waves are well recorded on long-period seismographs with suitable recording characteristics. This result was also clearly shown by Savino in his investigation entitled "The Nature of Long-Period (20 to 130 sec) Earth Noise and Importance of a Pronounced Noise Minimum to Detection of Surface Waves." The question of the importance of the nonpropagating component of atmospheric noise was also discussed in detail by Savino and will be considered here also.

If the longer period (> 30 sec) "noise" can be reduced, then higher magnification seismographs can be operated in the period range between 30 and 100 sec and the detection capability for earthquakes, at least, can be significantly improved.

INSTRUMENTATION

The seismological and microbarometric instrumentation which recorded the data used in this study were located at Sugar Island, Michigan.

The station is located in the northwest quarter of the southeast quarter of section 26, Township 48 N, Range 2 E. The geodetic location is 46°31'17" N, 84°08'18" W. The geocentric location is 45°44'54" N, 84°08'18" W. It is located 623 ft or 190 m above mean sea level on Cambrian Jacobsville sandstone. The Coast and Geodetic Survey code designation is SUG.

The seismic installation at Sugar Island consists of three Geotech (Model 7500 A and 8700 C) seismometers operated in pressure tanks at a period of 30 sec. One of the seismometer's velocity outputs is fed into a Geotech Photo Tube Amplifier with a 100-sec galvanometer and the amplified and filtered signal is recorded photographically and visually. The response curve for this output is shown in Figure 1. The other seismometer velocity output is recorded directly on photographic paper via a 100-sec galvanometer at a nominal gain of 6000. Displacement transducer outputs are amplified and recorded on 10-in. Esterline-Angus strip chart recorders.

Two NBS microbarographs are currently installed at Sugar Island. Response curves for these units are presented in Figure 2.

RESEARCH COMPLETED (1 FEBRUARY 1969 TO 31 JANUARY 1970)

The research carried out during this contract period was covered in Annual Report No. 1 on this contract and the results will be summarized here in accordance with the contractual requirements for a comprehensive final report. The results of the preliminary investigations showed that at La Paz, Bolivia, LASA/LAMA, Montana, and at Sugar Island, Michigan, there was a strong correlation between the microbarometric background noise and the long-period seismic noise. Furthermore, it was concluded that the energy transfer was the result of the deformation of the earth's surface by a nonpropagating pressure cell loading effect.

1. DATA ANALYSES—LA PAZ, BOLIVIA AND LASA/LAMA

For large amplitude propagating infrasonic waves from a presumed Lop Nor event as recorded at both sites, clear correlation between the seismic traces and the microbarometric traces was observed using "eyeball" filtering techniques and appropriate time shifting techniques. This correlation was observed on both the horizontal and vertical component seismic instrumentation and is undesirable. Dispersion curves for the atmosphere were derived from the LAMA microbarographs using standard seismological techniques.

2. DESCRIPTION OF MICROBAROMETRIC DATA—SUGAR ISLAND

Energy concentrations appear to be in four well-defined bandwidths: (A) 1-60 sec; (B) 60-300 sec; (C) 300-900 sec; and (D) greater than 900 sec.

A. Period Range 1-60 sec with peak amplitude at 40-50 sec. The waves of this group appear to be intimately connected with local wind action and are usually restricted to the time period between local sunrise and sunset. They reach a peak amplitude at approximately local noon and do not appear to be inhibited by cloud coverage. The high degree of correlation between solar noon and intense microbarometric noise suggests a thermal agitation of the local atmosphere as the probable cause.

B. Period Range 60-300 sec with peak amplitudes at 120-200 sec. The waves in this group occur quite prominently in two temporal bands on both sides of the first group at approximately 3 hr prior to local sunrise and local sunset. If they have large amplitudes, they are prominent later into the evening. Although they may be present during the time span of group A,

the greater amplitudes of the first group obscure these waves. These waves appear to be related to upper atmosphere solar setting and upper atmosphere turbulence as indicated by wind studies. These waves again appear to be independent of cloud coverage but are definitely temporal dependent as are the first group. There appears to be little or no correlation of these waves with very local meteorological conditions.

C. Period Range 300-900 sec with peak amplitudes at 300-420 sec. The waves in this band width, unlike the first two groups are not diurnally dependent, but occur to a greater or lesser extent throughout the records. They dominate quiet evening records and underlie both of the first groups. They appear to be related to low-pressure areas which pass over the station site. The more well developed the pressure field and the closer it is to the station, the larger the amplitude. Again, it appears that upper atmospheric conditions rather than those at the surface are the determining factor in the amplitudes. Work is being done to attempt correlation with jet stream and critical layer turbulence. The amplitude of these waves also appears to be temporally distributed with the season. Winter noise levels are noticeably larger.

D. Period Range Greater than 900 sec. These waves are rare but do occur occasionally with fairly large amplitudes. Fourier analyses indicate a power peak at approximately 1200 sec but amplification at these periods is not sufficient for significant results. On the records, dispersed waves are frequent occurrences and are not diurnally fixed. They occasionally transcend all other groups which sometimes distort the dispersion pattern. Dispersion of waves runs from periods of 25-30 min to 100-200 sec and generally occur over a finite interval of this limiting range. The correlation of these waves is as yet undetermined.

For convenience sake, in the discussion below, we have divided these energy concentrations into two period regions. These are 60-180 sec and 200-1000 sec. The characteristics of the two spectral regions are dissimilar and will be discussed separately below.

The first concentration of energy occurs with maximum amplitude at 100 sec. This is a diurnally variable spectrum apparently related to localized thermal convection cells. Characteristically from sunrise to local noon, there is a decrease in period (from 180 to 30 sec) and an increase in amplitude of the noise. After noon, the reverse is true, and evenings are virtually devoid of energy in this frequency range at Sugar Island. This condition occurs irrespective of areal cloud coverage. Direct thermal agitation of the

instrument is ruled out as a possible cause. Duplicate records are obtained from a transducer inside the thermally stable vault at Sugar Island, as opposed to outside. This is also true when the instrument is covered with snow.

Localized atmospheric convection cells are set up with the influx of infrared or ultraviolet radiation from the sun. The cells decrease in size and increase in coherency from morning till noon. This causes a decrease in period and increase in amplitude on the microbarographic records. The exact cell dimension has, as yet, not been determined.

The second frequency range (200-1000 sec) is, unlike the first, not a diurnal effect, but a grouping of gravity waves initiated by different phenomena as well as by low-pressure front activity. Particularly prominent periods associated with low-pressure areas are in the 5-10-min range. The amplitude of these waves appears to be a function of the coherency of the low-pressure area and proximity to the recording station. The period appears to be a function of pressure area dimensions and proximity.

3. CALCULATION OF ATMOSPHERICALLY INDUCED DEFORMATION

Calculations of the amount of vertical deformation of various half-space models have been made by several authors (Kuo; Burmister; Khorosheva). As a first approximation of the problem, the model for a simple half-space proposed by Khorosheva was used to calculate the amount of vertical deformation of the surface at Sugar Island. The pressure field is assumed to be centered at Sugar Island. Elastic parameters of a quartzite similar to that beneath the site were used for this calculation (Clark). Observed pressure was obtained from microbarograph data and pressure field dimensions and acoustic wave periods. Performing the calculation with the above parameters:

$$w = \frac{\lambda + 2\mu}{2(\lambda+\mu)} P_o R$$

where w = ground disp.
λ and μ = Lame constants
P_o = pressure
R = radius of pressure field

Vertical deformation on the order of 4μ is obtained. This value is quite close to the observed displacement and is in reasonable agreement with values reported by Savino. This is a reasonably close estimate to the actual ground displacement obtained since

A. the pressure field was not located directly over Sugar Island
B. pressure field dimensions are only crudely known
C. exact elastic parameters for Sugar Island are not determined

As a second approximation, a single-layered, half-space model proposed by Burmister was used. Elastic parameters for the first layer were those of a sandstone similar to the Jacobsville Formation at Sugar Island; the half-space remained the quartzite. Results from this calculation agreed with the first to within 20%.

4. CORRELATION DATA—SUGAR ISLAND

Initial calculations of the coherency and spectra of the Sugar Island seismic and microbarometric data were carried out during this period. Since the continuation of these studies constitute the principal portion of the research carried out during the following period (1 January 1970 to 30 May 1971), these preliminary results will only be mentioned here. Half-hour length segments of both types of data were Fourier analyzed. The similarity and simultaneous increase in level of the power spectra for the seismic and microbarometric data indicated that the "noise" was related. Although correlation of the two types of "noise" was indicated, the absolute correlation was believed to be limited by several factors.

A. Infrasonic acoustic noise is not a unique source of seismic noise in this band pass. At certain seasons, it constitutes 80-90% of the noise, while at other times, it makes up a smaller portion of the total.

B. The effects of the bedrock elasticity can cause extreme changes in the character of the noise between acoustic and seismic sensors. Phase, amplitude, and period characteristics may be altered.

C. As Hasselman pointed out, general excitation of an elastic layered half-space by a random (homogeneous and stationery) pressure response. Thus, it is necessary to consider both the local sources and the more distant acoustic sources.

D. The exact energy transfer mechanism to seismometers from acoustic phenomena is not clearly understood but is presumed to be (based on Savino's work at Lamont among others) actual ground deformation.

These results of these studies clearly indicated the need for additional detailed analysis of this and similar data. This "set the stage" for the next section of this study.

RESEARCH COMPLETED (1 FEBRUARY 1970 TO 31 MAY 1971)

1. DATA ANALYSIS

In the search for correlation between microbarograph fluctuations and seismicity, one of the primary problems is how to correctly apply statistical analysis techniques to two such partially nonstationary time series. This section discusses the methods used.

For successful statistical analysis of time series such as the sample records of microbarograph or seismic data, certain conditions must be met by the data. The most important of these is that they must be ergodic or stationary, i.e., parameters such as mean variance, autocorrelation functions, etc., are invariant in time. Observations of many phenomena do not completely satisfy this requirement and are known as "almost" stationary or weakly stationary. Variations in parameter estimate in these cases are represented by mean square errors.

Seismic and microbarograph variations for the periods of interest (10-100 sec) can be considered to be stationary or quasistationary. A complete justification of this assumption would require a study of the stability of the data as a function of period.

Quasistationary data can be investigated using standard statistical functions. The definitions of the most important of these functions are listed below.

2. MATHEMATICAL DEFINITIONS AND PROGRAMMING TECHNIQUES

The autocorrelation function, $R_{xx}(\tau)$, which describes the dependence of data at one time (t) on data taken at another time $(t+\tau)$, where τ is called the lag time, is obtained by taking the normalized average product $x(t) \cdot x(t+\tau)$. This will approach an exact autocorrelation function as the length of record, T, becomes very long.

$$R_{xx}(\tau) = \lim_{T\to\infty} \frac{1}{T} \int_0^T x(t)\, x(t+\tau)dt$$

The autocorrelation function is thus a powerful tool for detecting nonrandom effects in data which have a high random background.

The power spectral density function, $G_{xx}(f)$, which describes the frequency and amplitude composition of the data, is given for stationary data by

the Fourier transform of the autocorrelation function

$$G_{xx}(f) = 2\int_{\infty}^{\infty} R_{xx}(\tau)e^{-i\omega\tau}\,d\tau$$

These functions can be extended to apply to joint properties of two time series x(t) and y(t).

The cross-correlation function $R_{xy}(\tau)$ for two time series x(t) and y(t) is

$$R_{xy}(\tau) = \lim_{T\to\infty} \frac{1}{T}\int_{o}^{T} x(t)\, y(t+\tau)dt$$

The Fourier transform of the cross-correlation function is the cross spectral density function, $G_{xy}(f)$, given by

$$G_{xy}(f) = \int_{\infty}^{\infty} R_{xy}\, e^{-i\omega\tau}\,d\tau$$

The cross power at each frequency is the product of the corresponding amplitudes in the two time series. If a spectrum component is absent from either series, it will be absent from the cross spectrum. The phase angle associated with each frequency component of $G_{xy}(f)$ is the phase difference between equivalent components of the two time series.

In practice it is preferable to use the normalized cross power function or the coherence $\gamma^2_{xy}(f)$

$$\gamma^2_{xy}(f) = \frac{(G_{xy}(f))}{(G_x(f)\; G_y(f))} \leq 1$$

The functions determined from several finite series of data differ from the ideal ("true") estimates obtained from infinite series of data. The differences are represented by mean square errors which are usually inverse functions of record length and, at high frequencies, also of the sampling interval (Bendat and Piersol).

If a time history u(t) is sampled at N data points with a sample interval "h" between values, then the sample mean $\bar{u}$ is given by

$$\bar{u} = \frac{1}{N}\sum_{n=1}^{N} u_n$$

To simplify calculations, the mean value $\bar{u}$ is usually subtracted from all data. A time history x(t) is defined by

$$x_n = u_n - \bar{u} \qquad n = 1,\ldots,N$$

If this is not done, the power spectral density function exhibits a large peak at zero frequency which distorts estimates at other frequencies.

A further correction may be needed to remove a slow linear trend in which case x(t) can be represented by

$$x(t) = u(t) - \bar{u} - \bar{\alpha}\left(t - \frac{T_r}{2}\right) \qquad 0 \leq t \leq T_r$$

where $\bar{\alpha}$ denotes the average gradient of u(t) with respect to t and T_r is the record length.

The estimated correlation function at a displacement (rh) where r is the lag number is

$$R_{xx}(rh) = \frac{1}{(N-r)} \sum_{n=1}^{N-r} x_n \, x_{n+r} \qquad r = 0,1,\ldots,m$$

The maximum lag, m, in an analysis determines the low frequency cut-off $(mh)^{-1}$ or bandwidth resolution, B_e, for the power spectral density function, the high frequency cut-off being the Nyquist frequency:

$$f_c = \frac{1}{2h}$$

A smoothed estimate of the power spectral density is obtained by a Hanning process (Blackman and Tukey) in which the values of $G_{xx}(f)$ are replaced by:

$$G_{xx}(0) \rightarrow 0.5G_{xx}(0) + 0.5G_{xx}(1)$$

$$G_{xx}(r) \rightarrow 0.25G_{xx}(r-1) + 0.5G_{xx}(r) + 0.25G_{xx}(r+1)$$

$$G_{xx}(m) \rightarrow 0.5G_{xx}(m-1) + 0.5G_{xx}(m)$$

A further adjustment to $G_{xx}(f)$ is the Parzen lag weighting function, D_r, which improves the accuracy of spectral estimates.

$$D_r = 1 - 6\left(\frac{r}{m}\right)^2 + 6\left(\frac{r}{m}\right)^3 \qquad r = 0,1,\ldots,\frac{m}{2}$$

$$= 2\left(1 - \frac{r}{m}\right)^3 \qquad r = \frac{m}{2},\ldots,m$$

$$= 0 \qquad r > m$$

The calculation of joint properties of two time series uses cross-correlation coefficients. Using series of data reduced to zero mean, the coefficients are

$$R_{xy}(rh) = \frac{1}{(N-r)} \sum_{n=1}^{N-r} x_n \, y_{n+r}$$

The cross-correlation function $G_{xy}(f)$ is generally a complex number.

Record length, sample interval and resolution bandwidth must be decided upon so that the best use of analysis is made at the frequencies of interest.

The normalized standard error ε is approximately

$$\varepsilon \sim \frac{1}{\sqrt{B_e T_r}}$$

3. CORRELATION OF MICROBAROGRAPH TO SEISMIC MEASUREMENTS

Microbarograph and seismic long-period analog measurements were recorded on paper charts continuously from late September, 1969, through March, 1970. Randomly selected sections of these records were digitized using a 105-sec digitizing interval on an Erwin digitizer and processed using the statistical techniques discussed previously.

The seismic records were selected at time when no earthquakes were apparently occurring and microseism activity was not excessive. The parallel microbarograph records were subjected to only one selection prerequisite, i.e., that the paper chart was not saturated.

The records selected, their times, and their dates, are listed in Table I.

TABLE I

TIME INTERVALS FOR WHICH MICROBAROMETRIC AND SEISMIC DATA WERE SELECTED FOR ANALYSIS

Date	Time Interval
September 29, 1969	1620-1720 Z
September 29, 1969	1720-1820 Z
September 29, 1969	1820-2020 Z
February 20, 1970	2144-2335 Z
March 1, 1970	1300-2100 Z
March 1, 1970	1300-1500 Z
March 1, 1970	1500-1700 Z
March 1, 1970	1700-1900 Z
March 1, 1970	1900-2100 Z
March 27, 1970	0230-0440 Z

The general frequency composition of the data was determined by the power spectrum density technique outlined previously. Some periodicities are apparent but owing to the now stationary characteristics of the data they must be regarded as tentative. Reliable estimates of these periodicities can only be obtained by time averaging the power spectra.

The power spectra for each of the microbarograph and seismic records selected, together with the phase and coherency between these records is shown in Figures 2 through 20. For each set, the sample interval was 1.5 sec (i.e., Nyquist frequency = 0.3 sec^{-1}). The minimum lag used in the autocorrelation function calculation was 5% of the record. This gives approximately 40 degrees of freedom (i.e., n = 40) to each spectral estimate. The mean square error ε in the spectral estimate is given by

$$\varepsilon^2 \sim \frac{2}{n} \sim \frac{1}{\beta \cdot T} \sim 0.05$$

where T is the record length and β is the sample interval.

4. DATA DISCUSSION AND RESULTS

The results of this work are presented in Figures 3 through 20. Rather than discuss the significance of each individual figure, the composite results

of the data analysis program will be given.

A. A pronounced minimum in the power spectral distribution in the period range 40 to 60 sec is observed in all the data. The spectra shown in the figures are uncorrected for instrumental response. When the seismic spectra are corrected for the response shown in Figure 1, the minimum is clearly present. This minimum, observed by Savino and others, occurs in the area of maximum response of the seismograph system. Since the system response is almost the inverse of the noise curve, the instruments are ideally suited for detection of surface waves in this period range. The choice of magnification curves was made by Hade and Pomeroy on the basis of observed noise at Ogdensburg. The seismic instruments are clearly not sensitive to microbarometric noise in this period range. The evidence for this can be most clearly seen in the data for March 1, 1970 (1500 to 1700 Z) (Figure 12) where a high level of barometric power occurs around 30 sec period and the seismic power is unaffected. The observed minimum in the noise curve is clearly an extremely important result from the standpoint of the detection of surface waves from small magnitude earthquakes and explosions and, as Savino has pointed out, will also allow the use of seismic surface wave discriminants for explosions and earthquakes at lower magnitudes.

B. Peaks in the seismic spectrum which correspond to propagating seismic noise are clearly present at periods of less than 30 sec (Figures 3,8,10,12, 14,16). No corresponding peaks in the barometer power spectrum are observed. In addition, the low coherency and the random phase associated with these signal peaks strongly suggest that there is no correlation between the microbarometric and the seismic data in this period range.

C. At periods greater than 60 sec, the degree of correlation between the seismic and the microbarometric data becomes less clear. In general, it is true (as was reported in Annual Report No. 1 on this contract) that rising levels of microbarometric power in this period range correspond to rising levels of power in the seismic data in the same period range as in Figures 3,8,12, and 18. It should be noted here again that both the microbarometric and the seismic power spectrum are uncorrected for instrument response. The simultaneous increase in power on both sets of instrumentation clearly indicates a genetic relationship between the two data sets. However, it is equally clear that a one-to-one correspondence does not exist. The coherency values tend toward zero in this frequency range indicating almost no coherence between the recorded microbarometric signal and the seismic data. The microbarometric data is, however, recorded only immediately above the seismometer vault and thus constitutes simply a point measurement in space. It is probably true that the local earth deformations and tilts caused by the atmospheric loading effect are the result of average surface loading over an area at least 10 km in diameter. Thus to obtain a highly coherent set of data, an array of microbarometric measurements over the area encompassed by the 10-km diameter should be averaged. Initially, it was felt that such an experiment

could be carried out using the LASA/LAMA data. The wavelengths of the data, the small dimensions required, and the large dimensions of LAMA precluded this study. A study using an array of microbarometric sensors spread around the location of a high-gain, wide-band, long-period seismograph system would provide a definite answer to the coherency problem.

D. The data on the phase of the two signal sets indicates a trend toward 0 (i.e., waves in phase) at the very long periods (> 100 sec). At shorter periods, the phase data is highly variable, again indicating, as with the coherency, a low direct correlation between the microbarometric data (at one point) and the long period seismic noise.

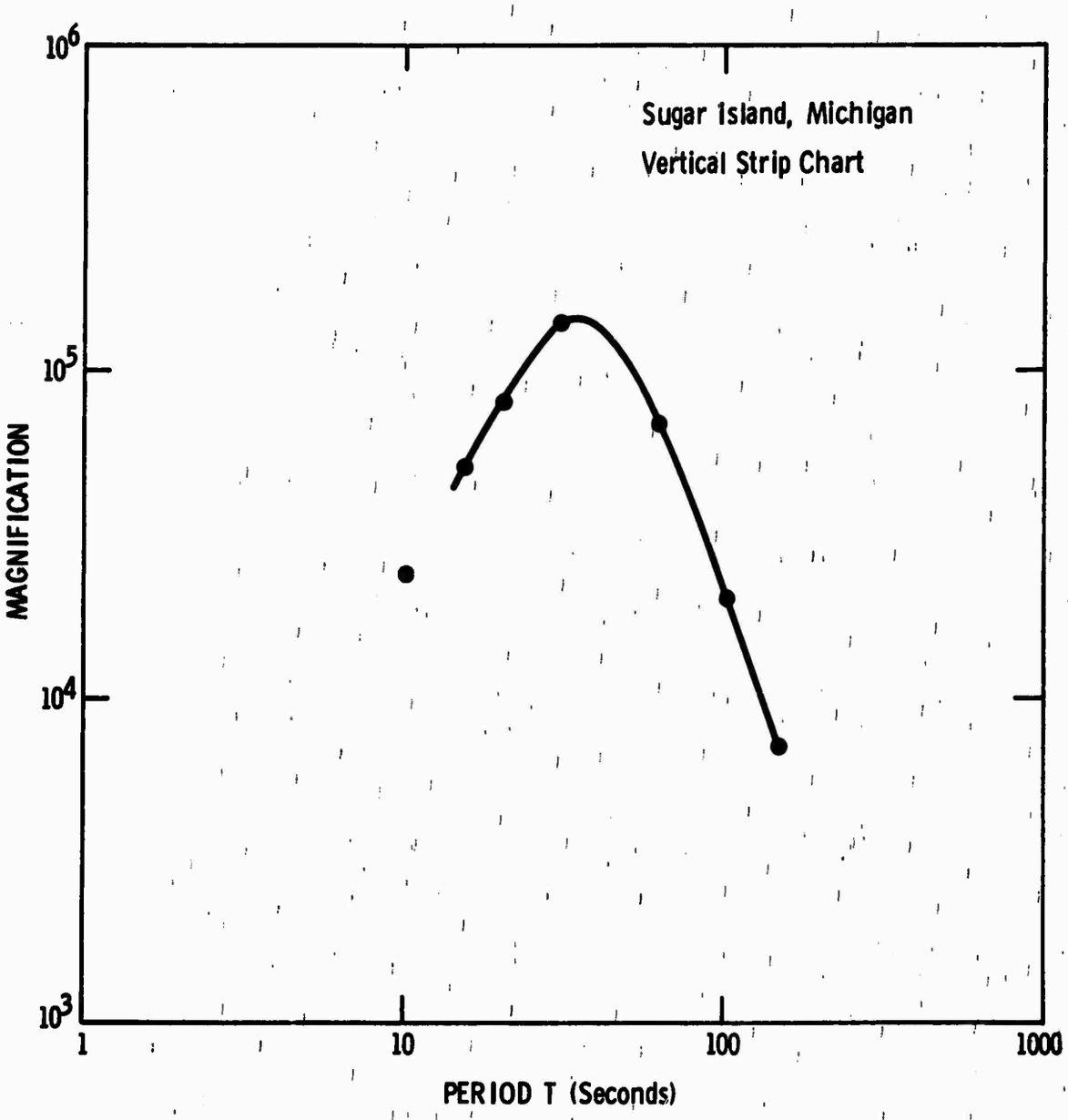

Figure 1. Response of long-period vertical component seismograph located at Sugar Island, Michigan.

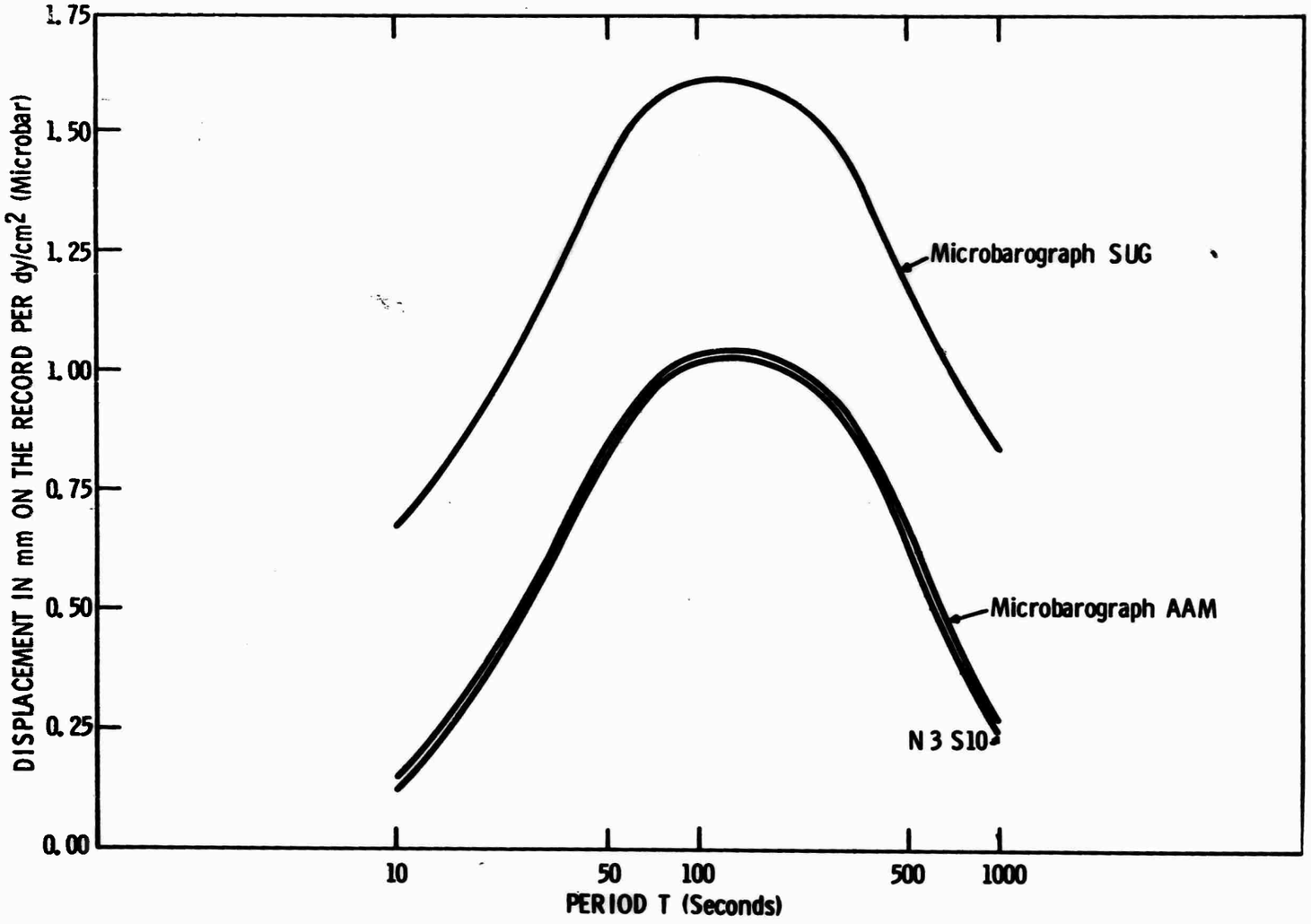

Figure 2. Response of long-period microbarograph located at Sugar Island (top curve).

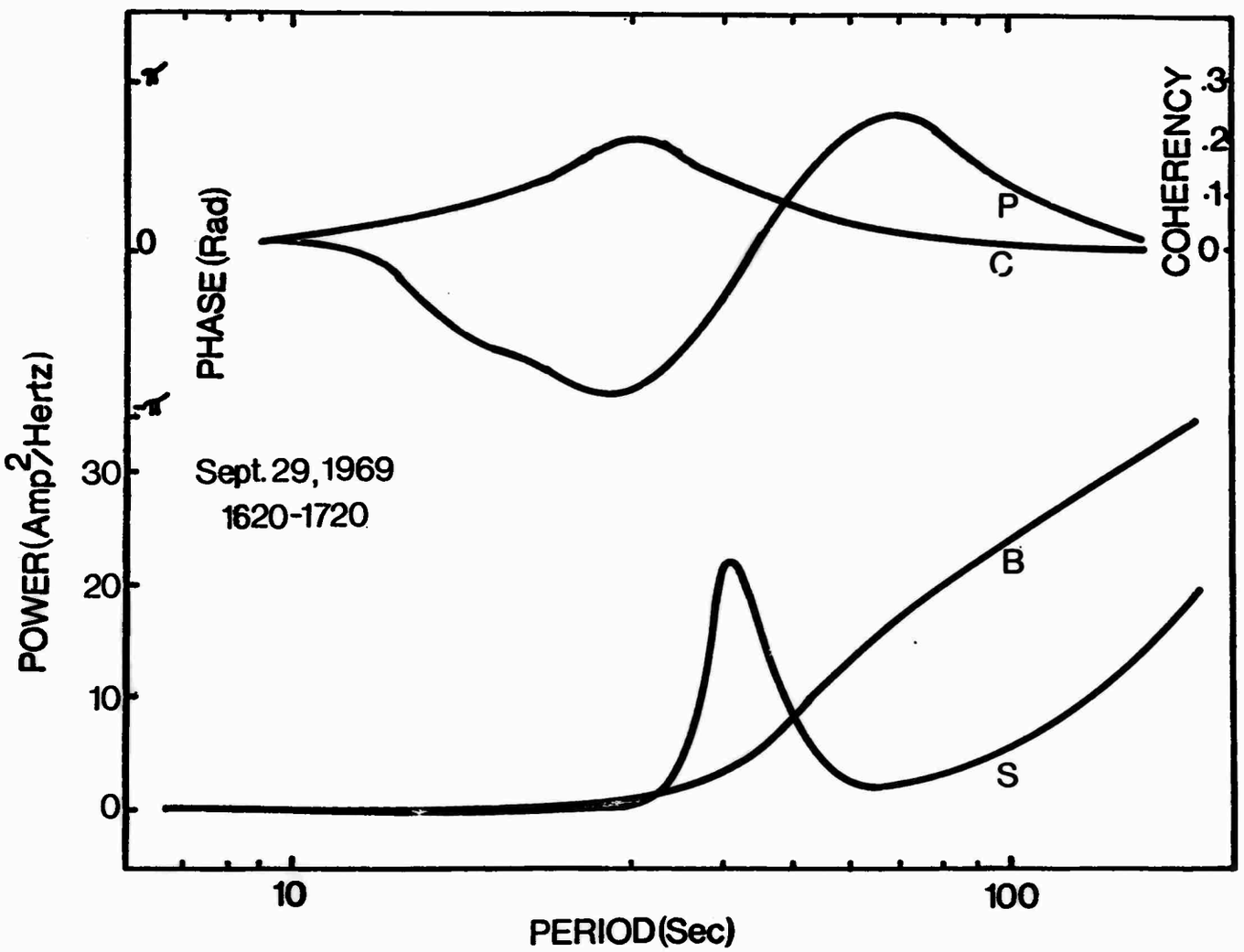

Figure 3. Spectra of microbarometric and long-period seismic data including phase and coherency spectrums for the period 1620 to 1720 Z on September 29, 1969. B indicates barometric spectrum; S indicates seismic spectrum; C indicates coherency spectrum; and P the phase spectrum. All spectra are uncorrected for instrumental response. Lower zero spectral values in this and subsequent figures should be disregarded since they are outside the range of this analysis.

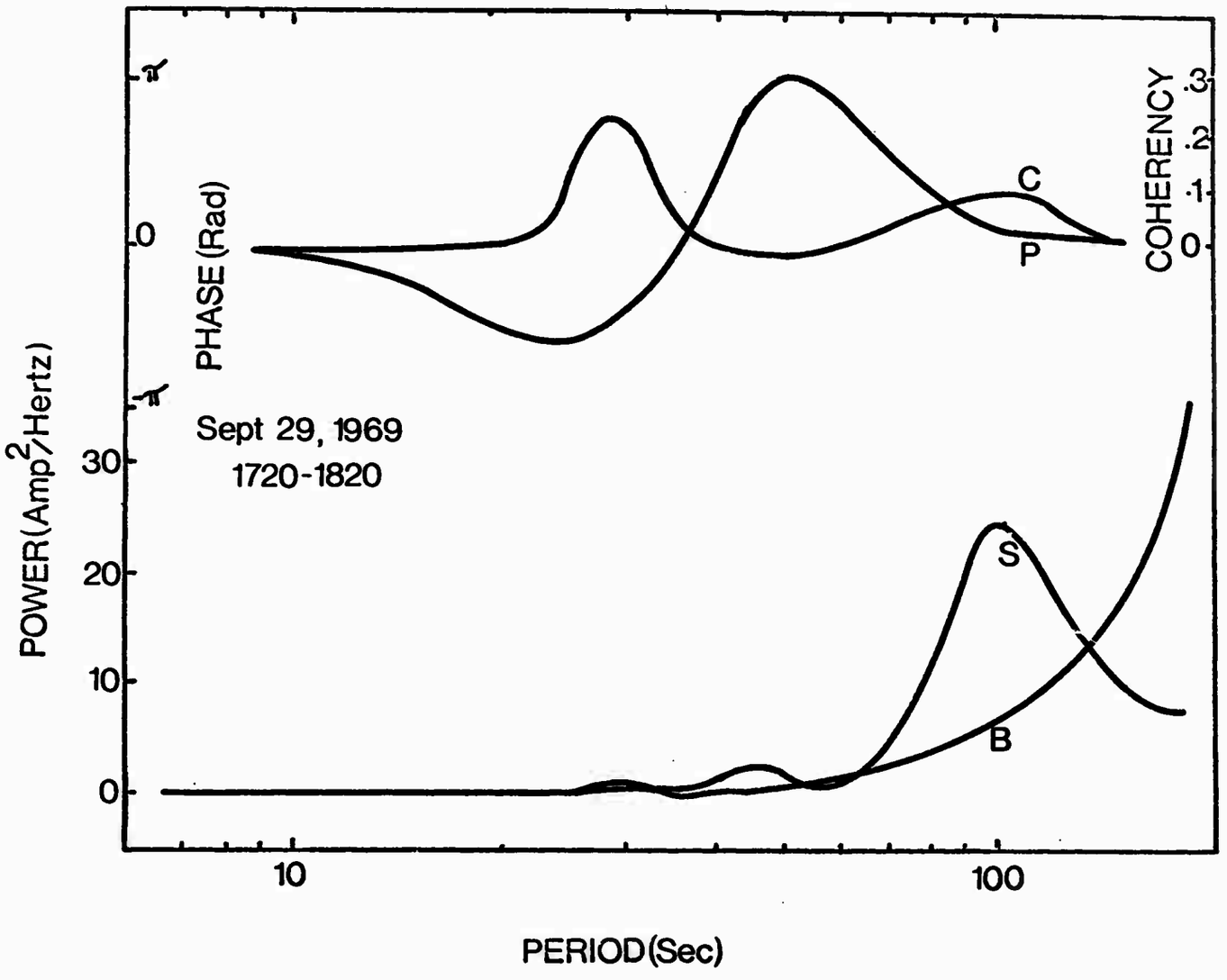

Figure 4. Spectra of microbarometric and long-period seismic data for the period 1720 to 1820 Z on September 29, 1969.

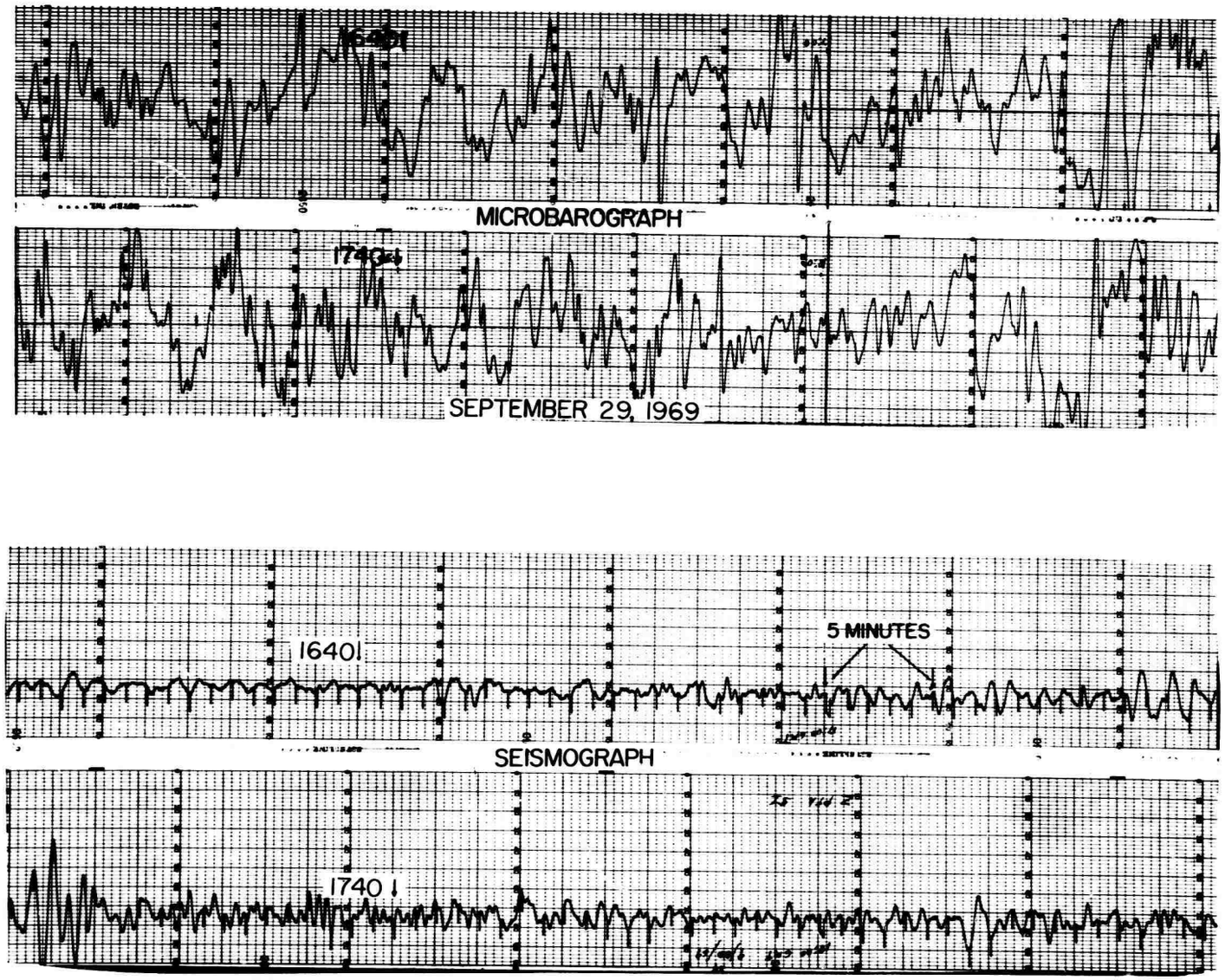

Figure 5. Seismic and microbarometric data used in the analysis illustrated in Figures 3 and 4.

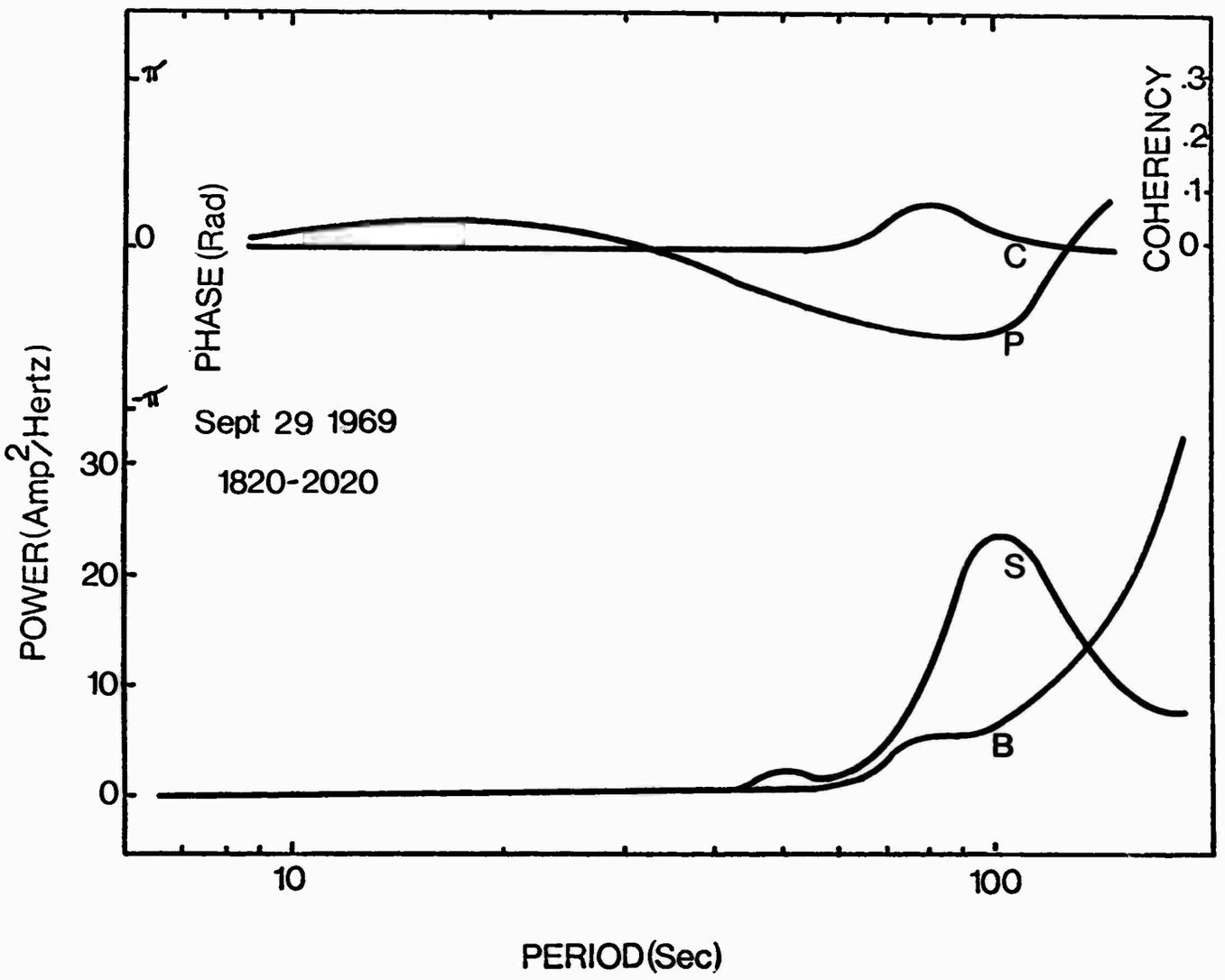

Figure 6. Spectra of microbarometric and long-period seismic data for the period 1820 to 2020 Z on September 29, 1969.

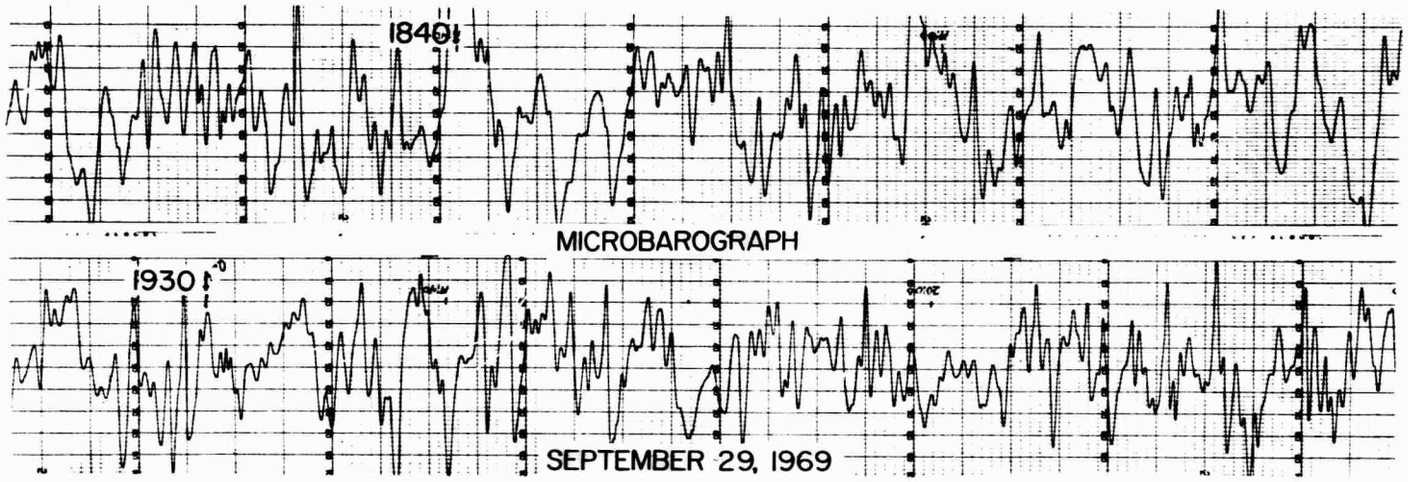

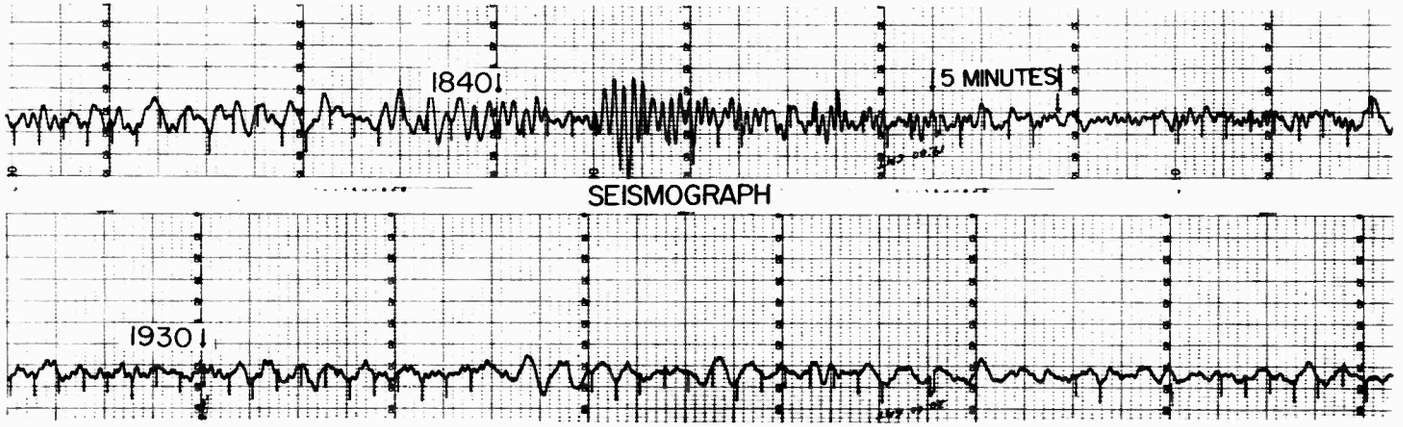

Figure 7. Seismic and microbarometric data used in the analysis illustrated in Figure 6.

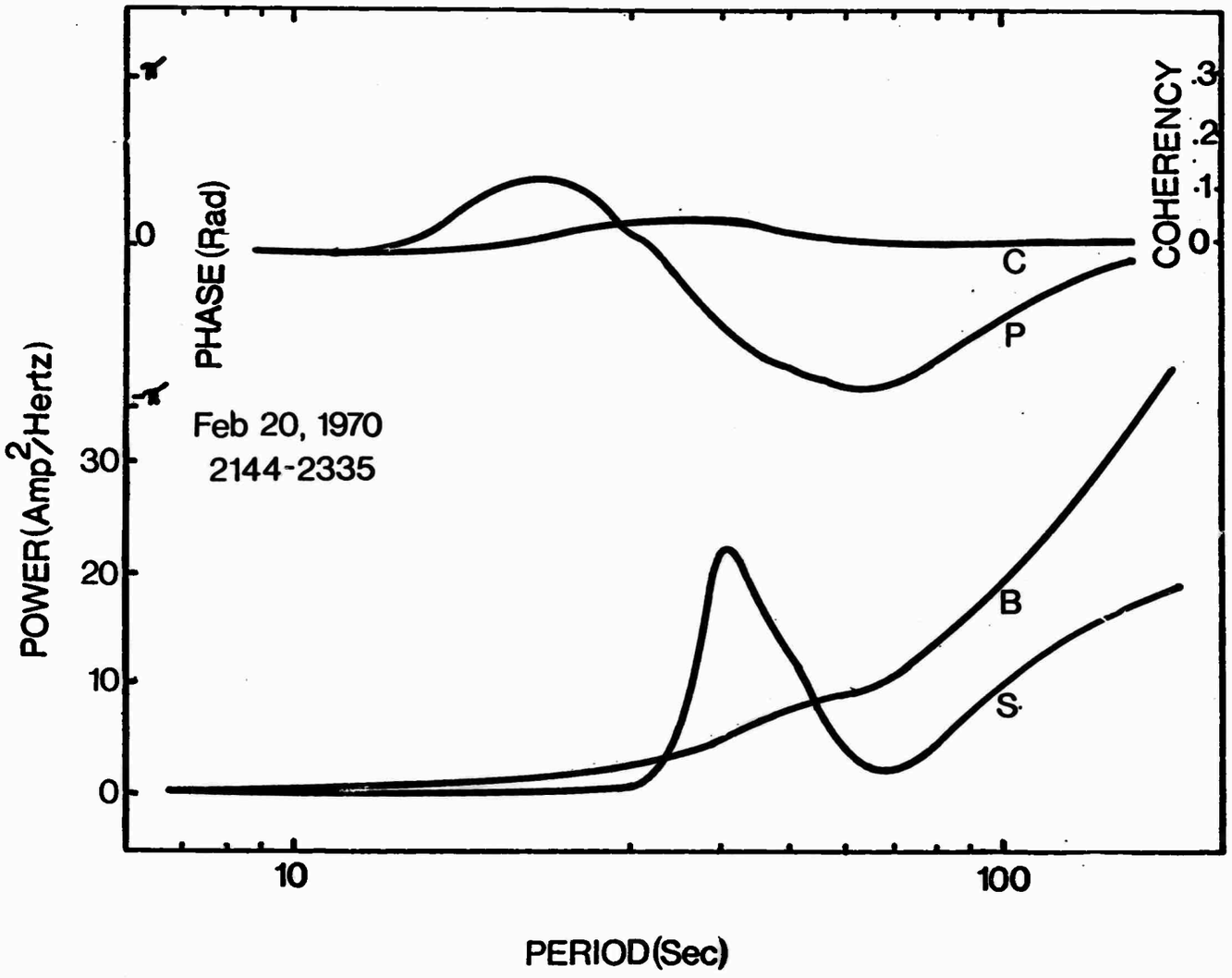

Figure 8. Spectra of microbarometric and long-period seismic data for the period 2144 to 2335 Z on February 20, 1970.

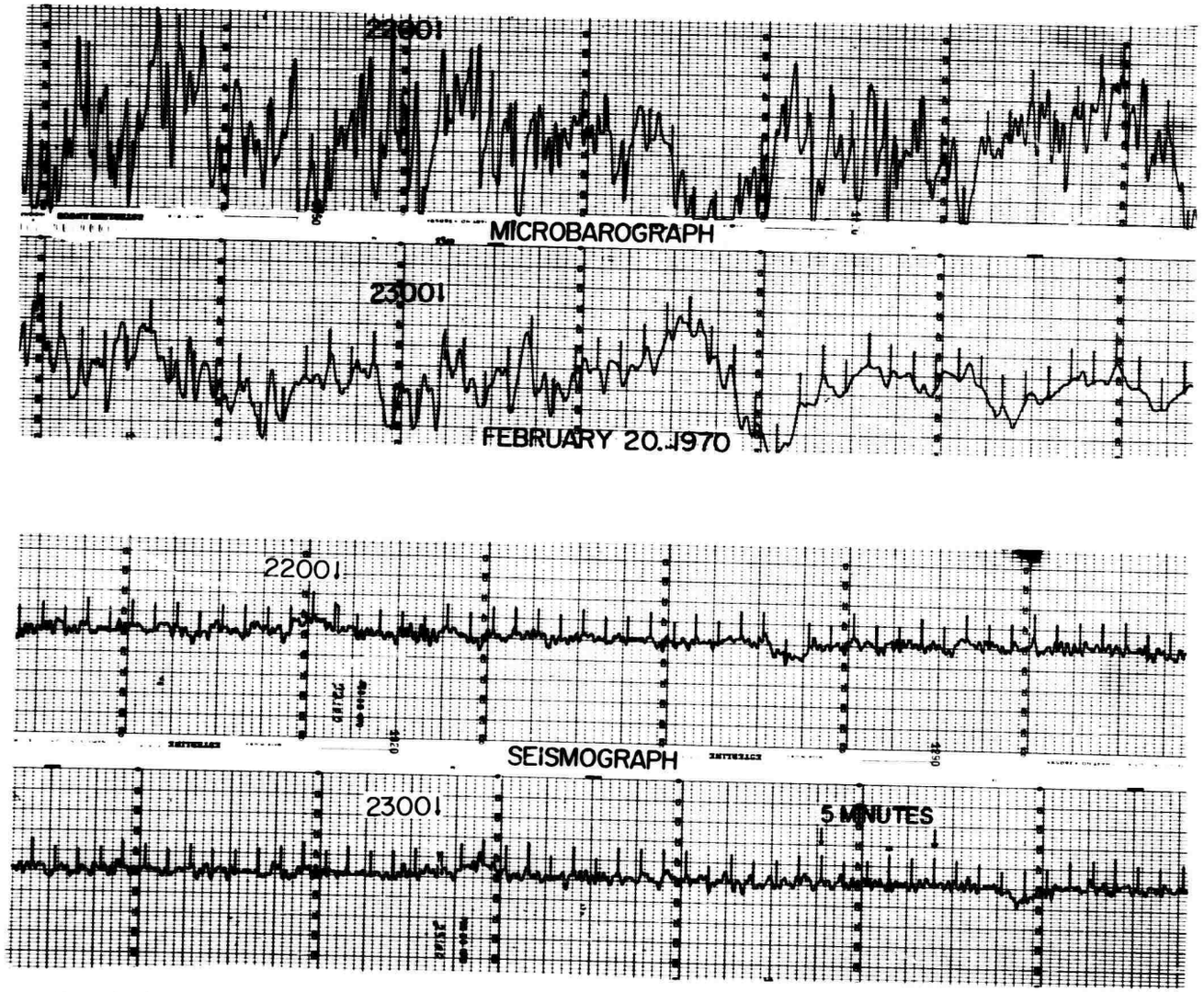

Figure 9. Seismic and microbarometric data used in the analysis illustrated in Figure 8.

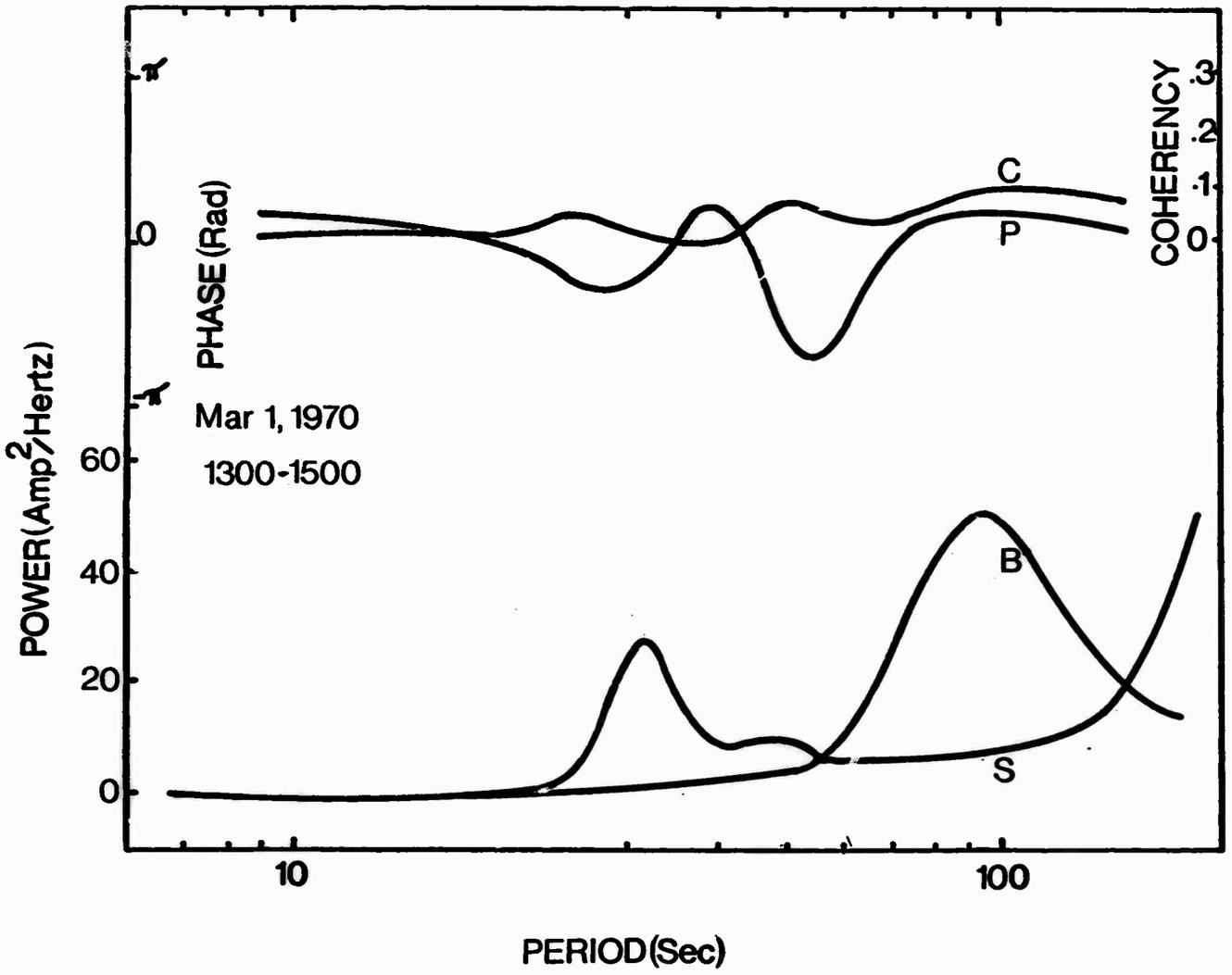

Figure 10. Spectra of microbarometric and long-period seismic data for the period 1300 to 1500 Z on March 1, 1970.

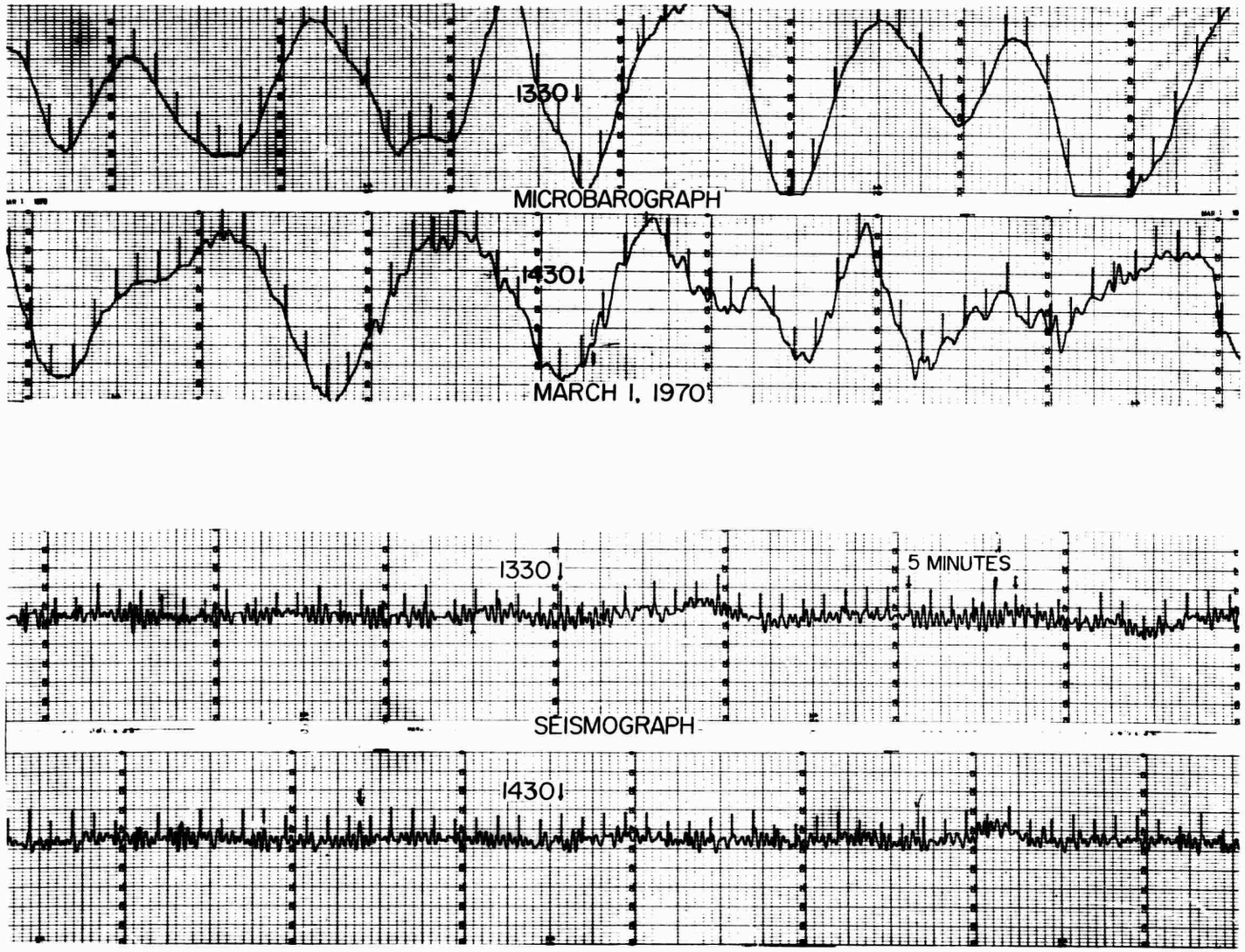

Figure 11. Seismic and microbarometric data used in the analysis illustrated in Figure 10.

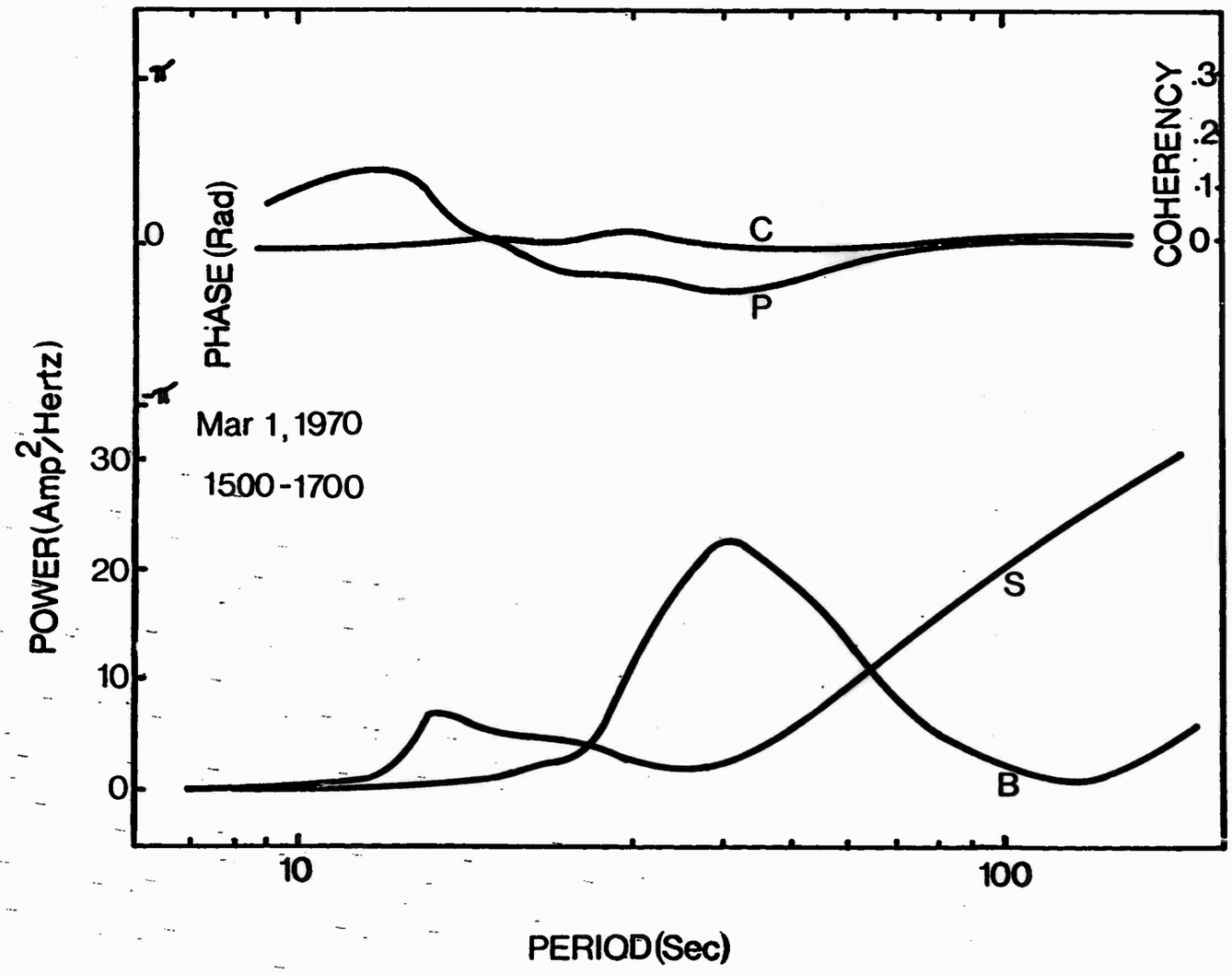

Figure 12. Spectra of microbarometric and long-period seismic data for the period 1500 to 1700 Z on March 1, 1970.

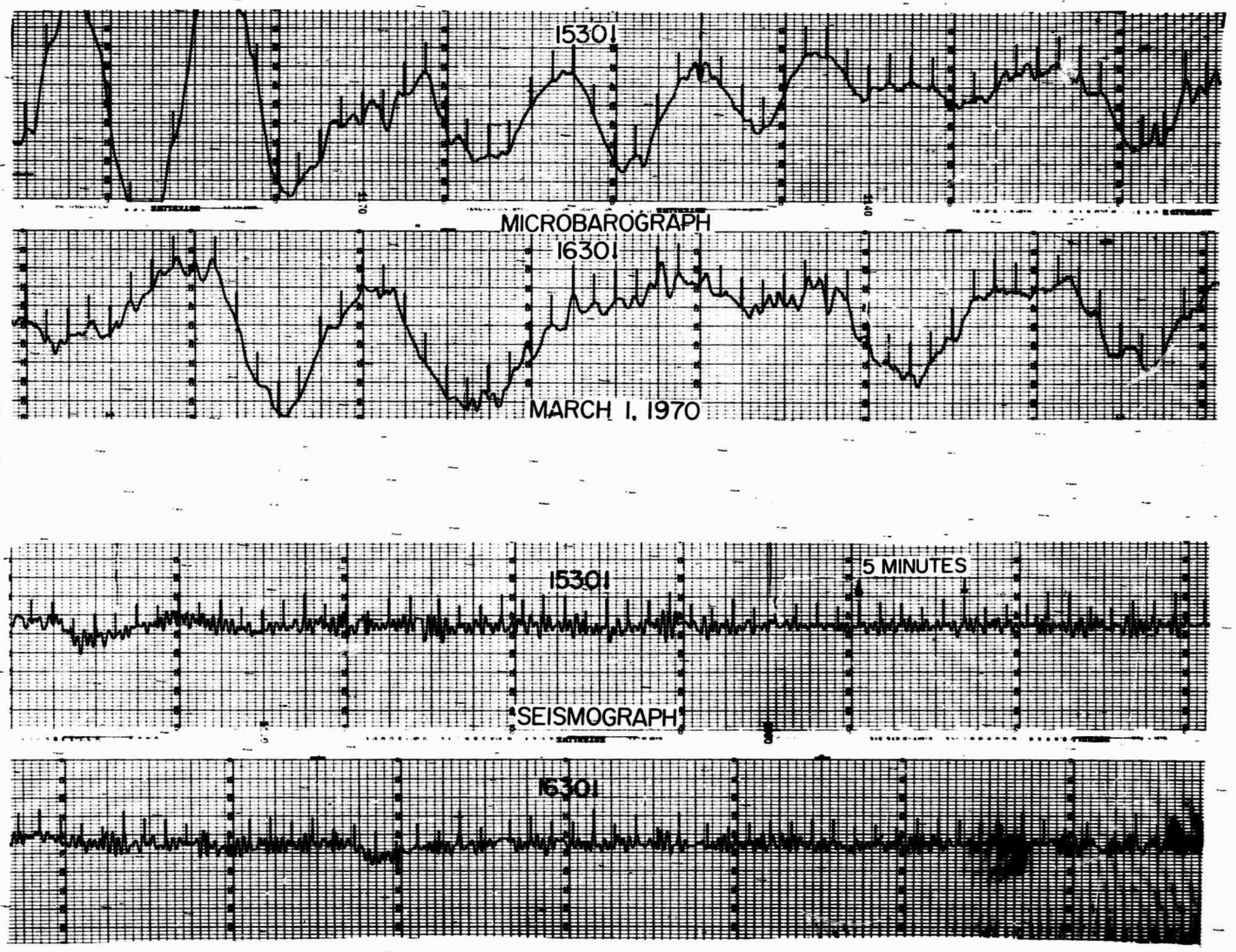

Figure 13. Seismic and microbarometric data used in the analysis illustrated in Figure 12.

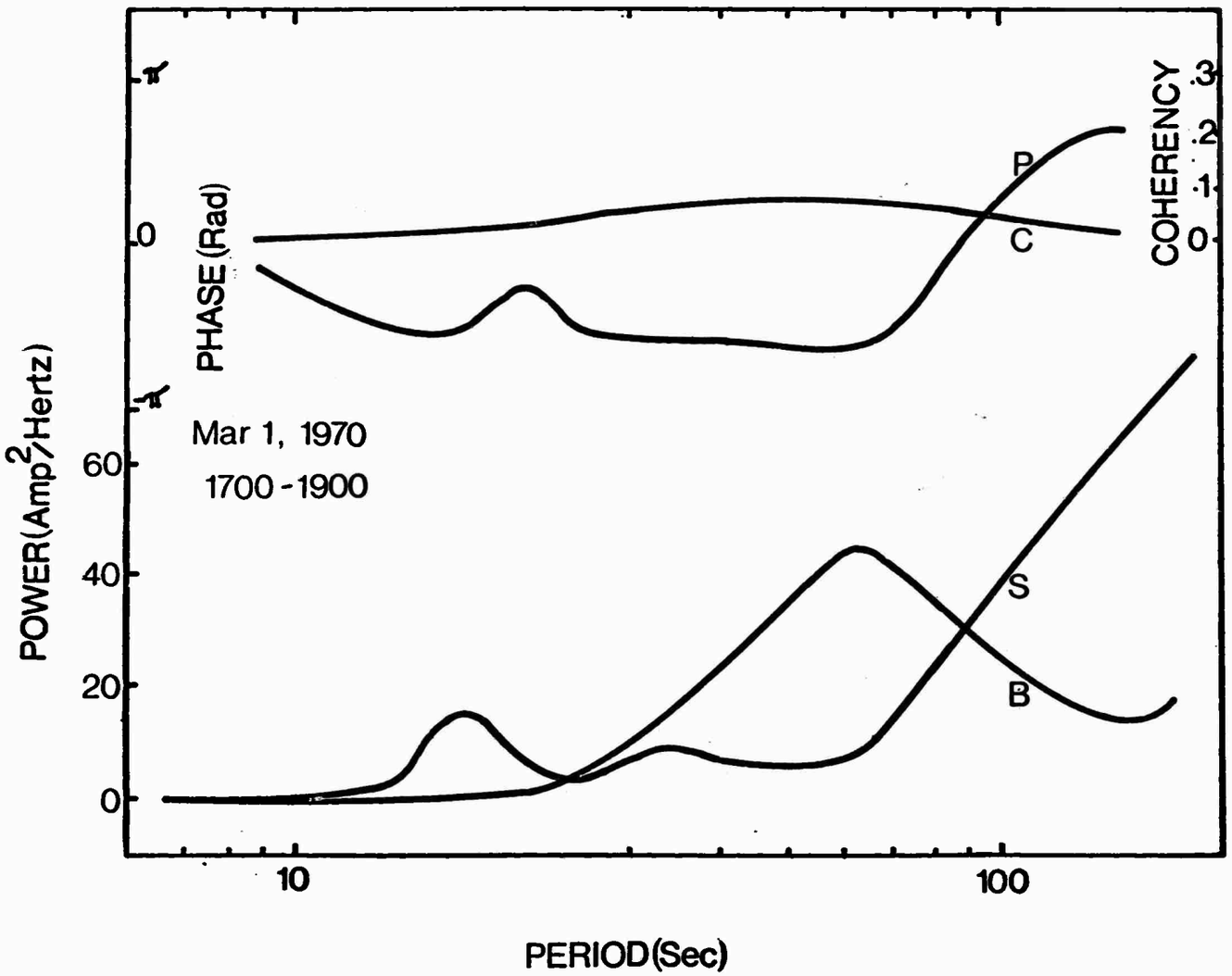

Figure 14. Spectra of microbarometric and long-period seismic data for the period 1700 to 1900 Z on March 1, 1970.

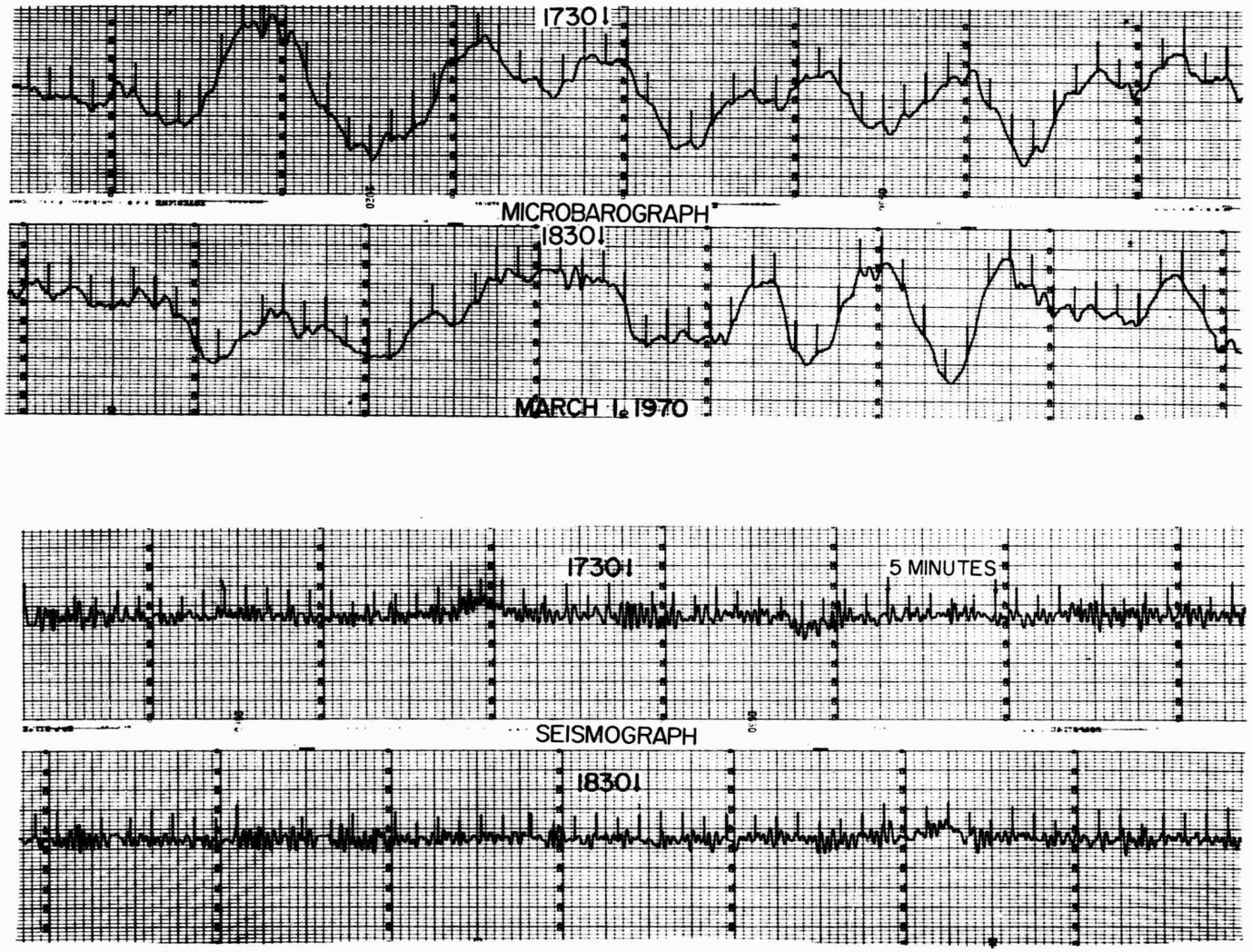

Figure 15. Seismic and microbarometric data used in the analysis illustrated in Figure 14.

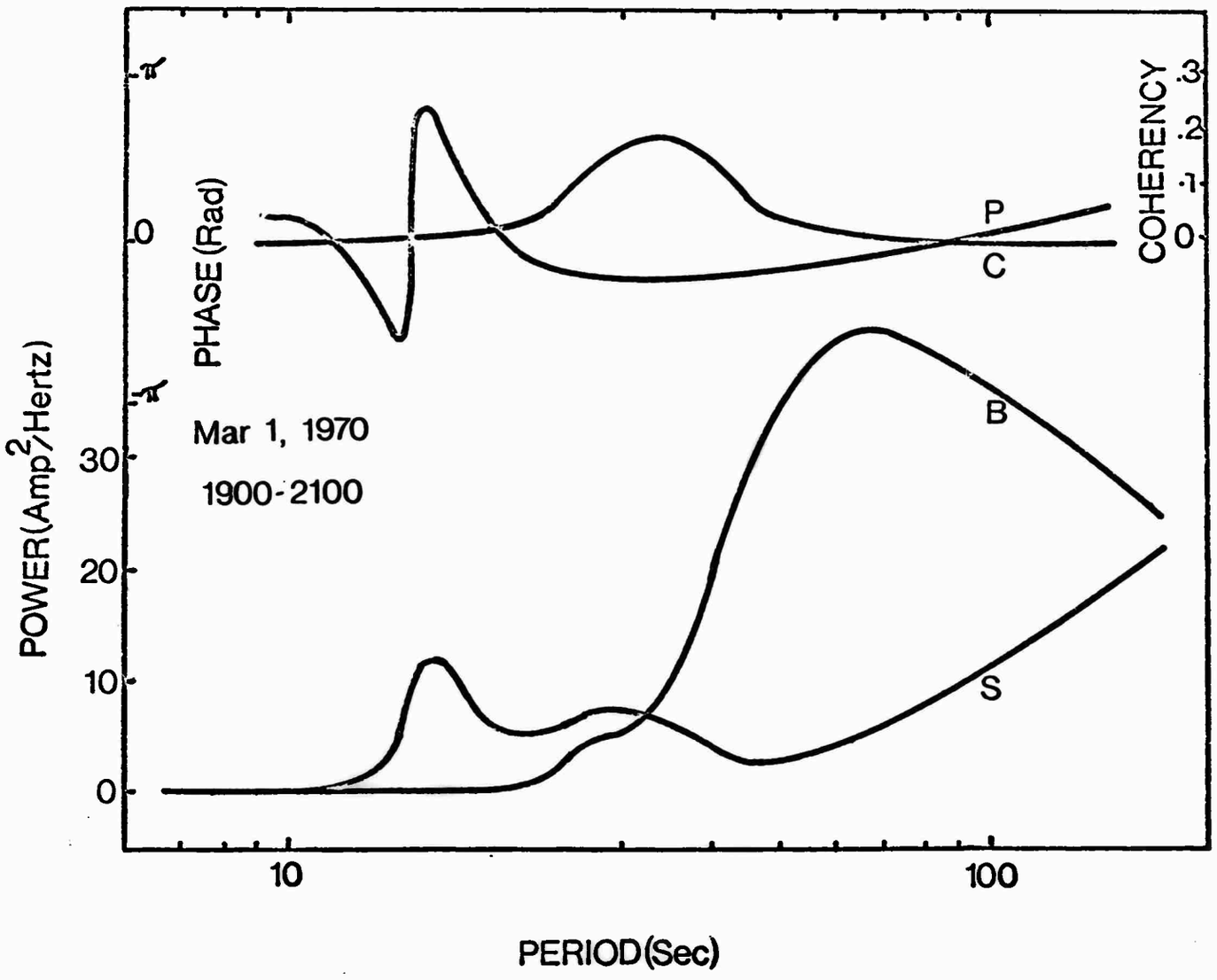

Figure 16. Spectra of microbarometric and long-period seismic data for the period 1900 to 2100 Z on March 1, 1970.

Figure 17. Seismic and microbarometric data used in the analysis illustrated in Figure 16.

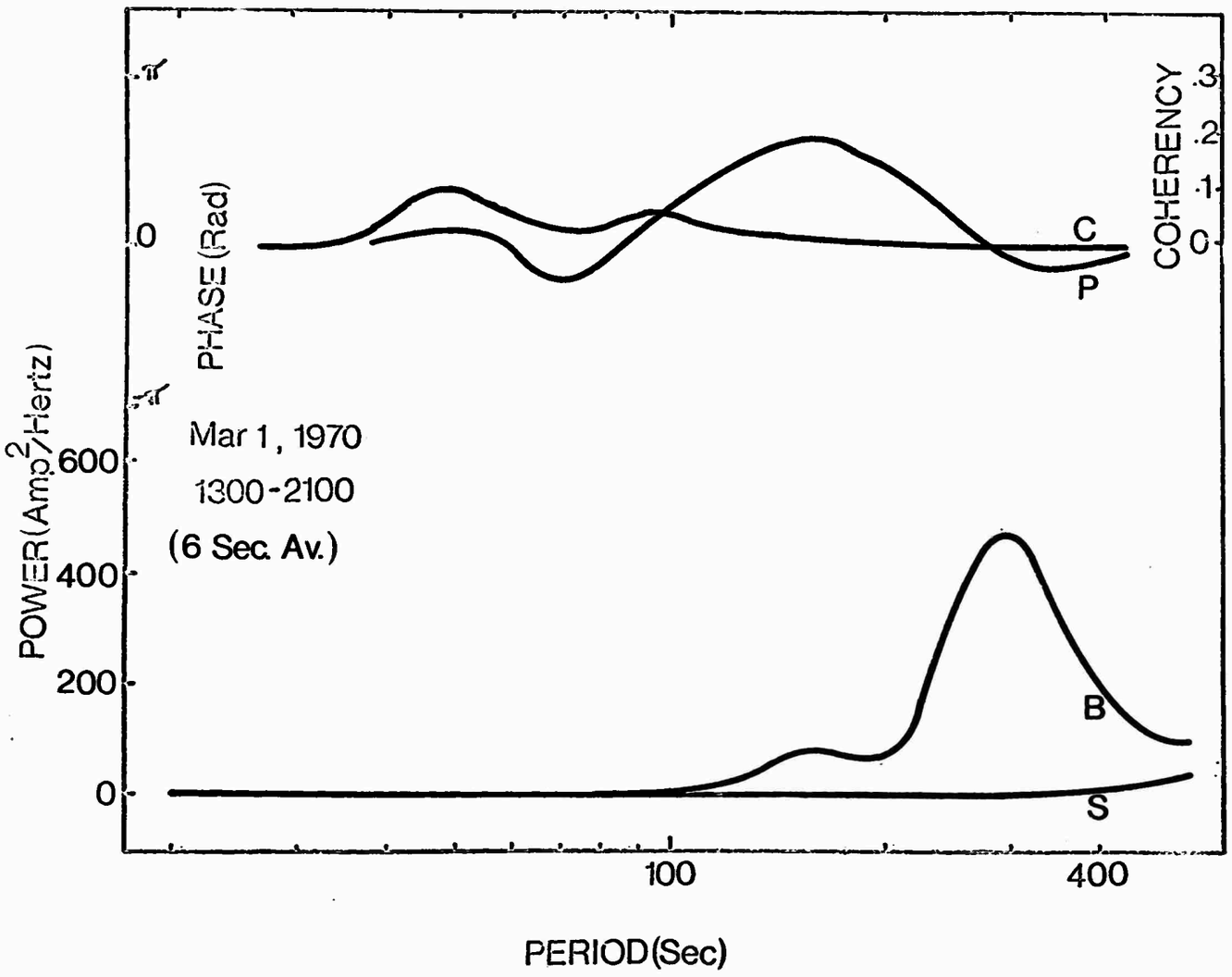

Figure 18. Spectra of microbarometric and long-period seismic data for the period 1300 to 2100 Z on March 1, 1970. Six-second averaging used on the data.

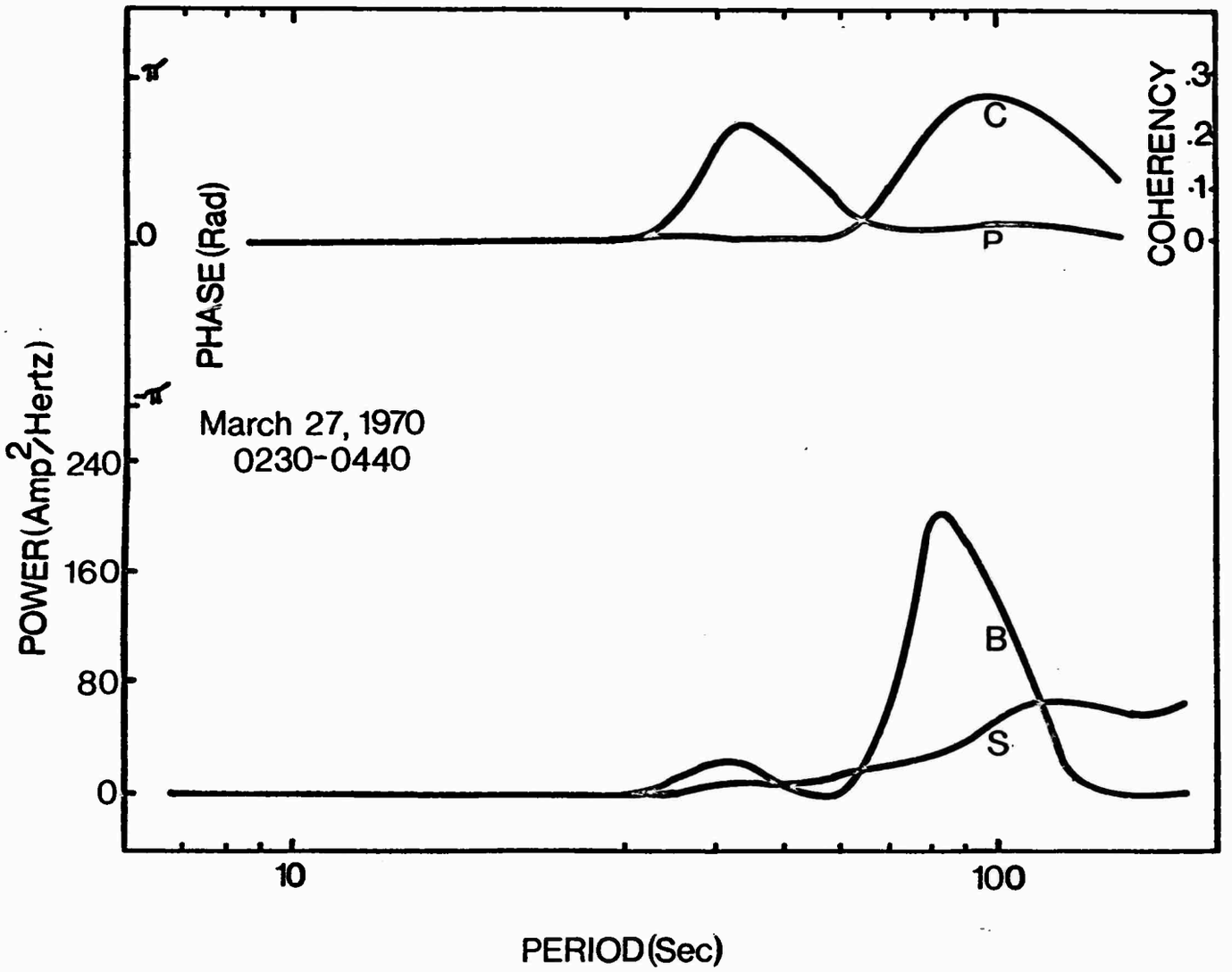

Figure 19. Spectra of microbarometric and long-period seismic data for the period 0230 to 0440 Z on March 27, 1970.

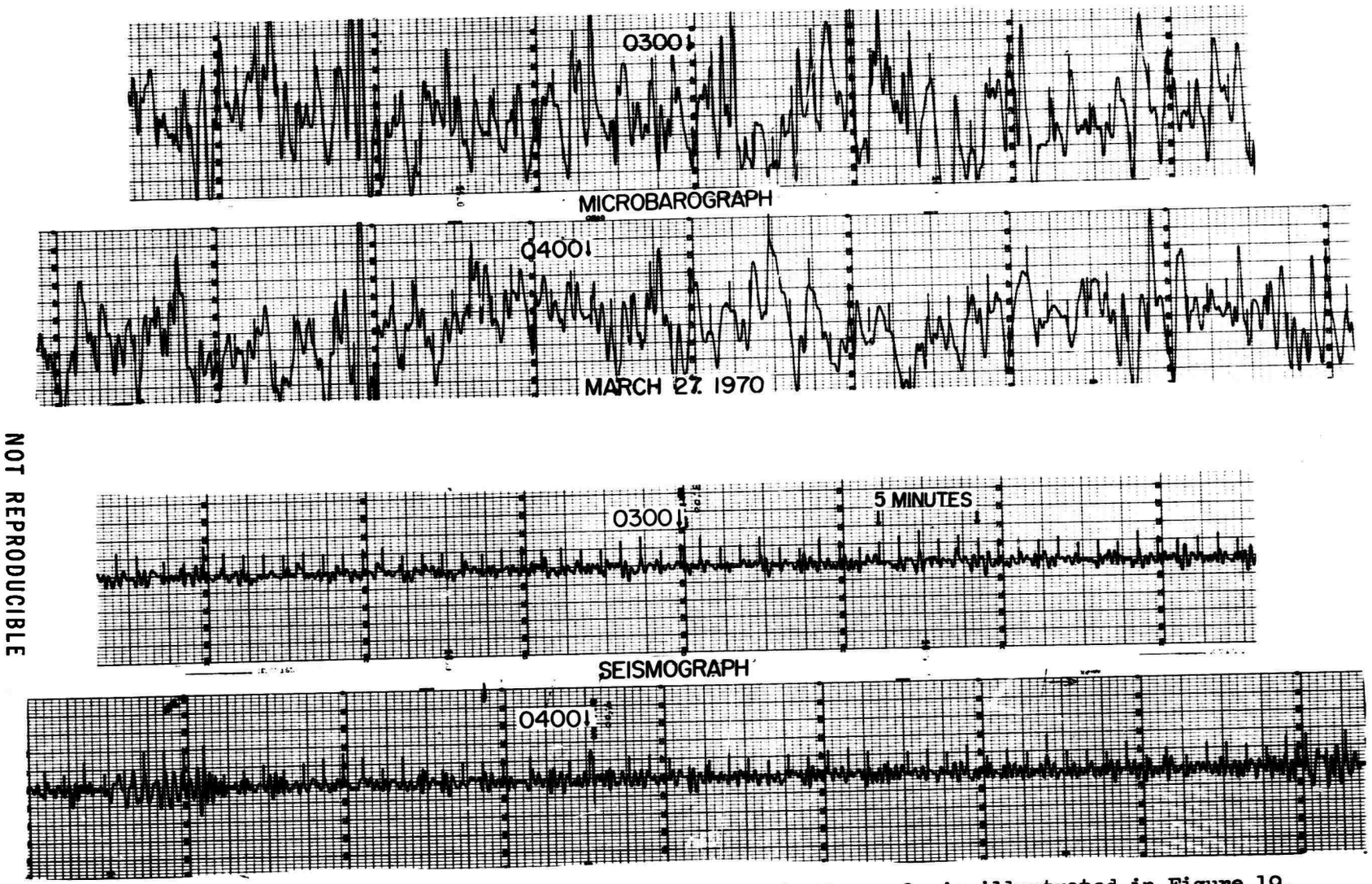

Figure 20. Seismic and microbarometric data used in the analysis illustrated in Figure 19.